Energy & Buildings 298 (2023) 113525

Contents lists available at ScienceDirect

Energy & Buildings

journal homepage: www.elsevier.com/locate/enb

Design recommendations for the rehabilitation of an urban canyon in a subtropical climate region using aerial thermography and simulation tools

Marta Videras Rodriguez [a], Sergio Gomez Melgar [b,*], Jose Manuel Andujar Marquez [b]

[a] Programa de Doctorado de Ciencia y Tecnología Industrial y Environmental, Centro de Investigación en Tecnología, Energía y Sostenibilidad, CITES (Research Centre for Technology, Energy and Sustainability), Universidad de Huelva, Campus El Carmen, 21071 Huelva, Spain

[b] TEP192 Control y Robótica, Centro de Investigación en Tecnología, Energía y Sostenibilidad, CITES (Research Centre for Technology, Energy and Sustainability), Universidad de Huelva, Campus El Carmen, 21071 Huelva, Spain

ARTICLE INFO

Keywords:
Urban thermal comfort
Canyon street
Predicted Mean Vote (PMV)
Predicted Percentage of Dissatisfied (PPD)
Unmanned aerial vehicle (UAV)
Aerial thermography
ENVI-met

ABSTRACT

Outdoor public space is the setting for everyday social interaction where activities take place in order to satisfy collective urban needs. It is important to achieve climate-friendly urban design in order to ensure acceptable urban thermal comfort, especially in over-urbanised city centres during summer periods. In this research, an urban canyon street located in the historical centre of the subtropical city of Huelva (Spain) was analysed. After a survey carried out by in situ meteorological sensors and airborne infrared sensors (equipped on an unmanned aerial vehicle, UAV), the current thermal comfort was analysed in terms of PMV and PPD at different times of a typical summer day (11:00 h, 15:00 h and 19:00 h) with the aim of formulating design recommendations to improve its performance in terms of urban comfort. Then, thermal comfort was evaluated in different scenarios where feasible mitigation strategies (replacement of materiality, addition of vegetation and sun shading elements) were applied to classify them according to their effectiveness using the ENVI-met simulation tool. The results of the current scenario showed that, due to its N-S orientation and its aspect ratio (H/W), the urban comfort depends drastically on the day hour variation. A comfortable thermal environment is achieved at all points of the urban canyon as a result of the shade generated by the buildings during the morning and afternoon. However, in the central hours of the day the feeling of thermal discomfort was alarming (PMV values of +3 and PPD values above 90%). The proposed mitigation measures showed a considerable improvement in urban thermal comfort, with the addition of vegetation being the most effective solution (with an improvement in PMV value of 42% and a reduction in PPD value of 43%). The combination of all the proposed measures in a single scenario showed encouraging results in the rehabilitation of public spaces in use.

1. Introduction

The street is the boundary between the architectural scale and the urban scale as it connects buildings and the city. It is therefore a determining element in the energy efficiency of buildings as it directly affects their interior microclimate and can influence their energy consumption. It is also a determining factor in terms of urban sustainability, as street design also affects urban thermal comfort conditions.

Studies related to urban thermal comfort problems generate valuable information for urban planners and architects [1], as the data and suggestions obtained contribute to the design process for better and healthier urban environments. This type of human bioclimatological studies have a specific importance if they are carried out in summer due to the influence of the urban heat island effect that remains longer after sunset and intensifies generating a high thermal stress during the day [2]. This urban heat island effect directly affects the local climate of urban spaces, especially in city centres, causing an increase in urban temperature mainly due to the structure, materials and general lack of vegetation in modern cities. This may cause discomfort and even some danger to human health, especially in cities with hot climates [3].

The scientific community has developed multiple models to estimate the energy balance between the human body and the surrounding environment in order to quantify urban thermal comfort. Such models are based on rational indices, proposed at the end of the 20th century, determined by solving the human energy balance equation: predicted mean vote (PMV) [4], predicted percentage of dissatisfied (PPD) [5],

* Corresponding author.
E-mail addresses: marta.videras245@alu.uhu.es (M.V. Rodriguez), sergomel@uhu.es (S.G. Melgar), andujar@uhu.es (J.M.A. Marquez).

https://doi.org/10.1016/j.enbuild.2023.113525
Received 28 May 2023; Received in revised form 16 August 2023; Accepted 6 September 2023
Available online 7 September 2023

physiological equivalent temperature (PET) [6], standard effective temperature (SET, also called OUT_SET) [7], universal thermal climate index (UTCI) [8], among others (Table 1).

Calculating these indices requires measurements of meteorological factors that affect human comfort such as air temperature, wind speed, relative humidity and the short-wave and long-wave irradiances that impact on a person from the surrounding environment, i.e the mean radiant temperature. Other indices focused on specific climates, such as the MOCI index (Mediterranean Outdoor Comfort Index) was proposed for Mediterranean climates [25,26]. In the 2000s, early research studying outdoor thermal comfort usually used the PET index [14–19] while PMV was used to estimate the thermal comfort of indoor spaces [27–30]. Although many of the above-mentioned indices were developed for indoor conditions (such as PMV and SET), they were later reformulated for application in outdoor studies [31].

In recent years, the scientific community has been evaluating the strong influence of densely built urban areas on the formation of urban climate conditions in order to determine the factors contributing to urban thermal stress. On the development of a comfortable microclimate for pedestrians in urban canyons, methodologies based on in situ meteorological data acquisition in combination with simulation tools have been mainly used to study various urban design scenarios [32–37]. Using simulation tools, such as the ENVI-met software, the influence of different urban design parameters, such as orientation and aspect ratio (height-to-width ratio, H/W), in urban canyons in a hot and dry climate was analysed [18]. The importance of the aspect ratio was demonstrated in subtropical latitudes where small values such as H/W = 0.5 ensure a thermally stressed environment regardless of its orientation, indicating that aspect ratios higher than 2 are necessary for the generation of comfortable environments. It was also determined that urban canyons with W-E orientations are less thermally comfortable than those with N-S orientations for all H/W ratios in Mediterranean cities [38].

In subtropical climates, the street canyon orientation is the most influential factor (46.42%), followed by aspect ratio (30.59%) [39]. Orientation and aspect ratio are relevant because they are related to the direct solar exposure of the urban canyon. Direct solar radiation is a determining factor in the thermal comfort of the street because the higher is the temperature of the surrounding surfaces, the greater is the radiant energy dissipated. In wide urban canyons - of low aspect ratio - the air temperature is conditioned by the surface directly exposed to solar radiation. When comparing the surface temperature of a façade exposed to the sun and another façade without solar exposure in a typical canyon in a subtropical city, the heat transfer of the shaded walls was negligible in comparison with the sunlit walls [40]. The thermal behaviour of the materials and their effect on air temperature or relative humidity has also been studied using ENVI-met software [41].

Table 1
Summary of climate indices.

Index	Description	References in text
Predicted mean vote (PMV)	Determines the average thermal sensation of a group of people using the ASHRAE psychophysical scale.	[9–12]
Predicted percentage of dissatisfied (PPD)	Provides an estimate of the number of occupants of a space who would be dissatisfied with the thermal conditions.	[10,11,13]
Physiological equivalent temperature (PET)	Defines the air temperature at which, in a reference environment, the heat balance, skin and core temperatures are the same as those found in the given environment.	[6,14–19]
Standard effective temperature (SET, OUT_SET)	Indicates the air temperature at which, in a given reference environment, the person has the same skin temperature and the same humidity as in the real environment.	[7,20,21]
Universal thermal climate index (UTCI)	Describes the synergistic heat exchanges between the thermal environment and the human body, namely its energy budget, physiology and clothing.	[8,22–24]

In other cases, it was shown that the use of the urban canyon also influences the thermal comfort. Studying the thermal comfort of two urban canyons with the same orientation and aspect ratio in a Mediterranean city, the influence of heavy traffic was observed to increase the street air temperature by 2 °C [42]. The presence of vegetation and shading elements has been widely evaluated as a mitigation measure for reducing air temperature in urban spaces [43–46]. It was shown that covering roofs and walls of an urban canyon with vegetation not only significantly improves thermal comfort in cities with warm climates (reduction of air temperature higher than 6 °C), but also in cities with cold climates (up to 4 °C) [47]. In Mediterranean cities, ground and roof vegetation was shown to mitigate summer temperatures, decrease the cooling demand of buildings and improve urban thermal comfort. Ground vegetation proved to be more effective than roof vegetation in reducing the PMV of the urban canyon [48]. Covering pavements and walls, in this case with “cool coatings” i.e. reflective pigments that reflect light, in a Mediterranean urban canyon also showed a decrease in pavement surface temperature of up to 7–8 °C, facade surface temperature of 2–3 °C and air temperature of 1 °C [49].

Also in the rehabilitation of another Mediterranean urban canyon, the proposed solution combining cool roofs, urban vegetation and cool pavements led to a maximum decrease of the MOCI index of −2.5 and −3.5 with respect to the current site configuration [50]. The impact of sun sail-shading strategies in hot climates was studied and found that adding 60% or above sun shading in a courtyard results in a 0.6 reduction in average PMV [51].

Based on the literature review, it has been shown that urban thermal comfort depends on multiple factors: street geometry, aspect ratio, orientation, solar availability, traffic density, the presence of shading elements, vegetation, materiality etc. It has also been shown that the thermal environment of human and the energy flows between body and environment can be quantified on the basis of variations in air temperature or thermal indices such as PET, PMV, PPD, MOCI etc. by means of in situ measurements and simulation tools.

This paper aims to contribute to a better understanding of the thermal sensation of urban canyons using a novel methodology based on the use of thermography equipped in an unmanned aerial vehicle (UAV). UAVs have demonstrated to be an ideal technology due to their optimal performance in terms of time, precision, safety and cost [52]. Results of a numerical study are presented with the final objective of formulating design recommendations for the rehabilitation of an urban canyon in a subtropical climate region. The analysis was performed for different hours of a typical summer day and points out the spatial variations of human thermal sensation at street level, differentiating between the edges and the centre of the urban canyon. For this purpose, an in situ inspection was first carried out using remote sensing for obtaining values of air temperature, relative humidity and mean radiant temperature. The assessment of current thermal comfort was expressed by the predicted mean vote (PMV) and the predicted percentage of dissatisfied (PPD). Then, thermal comfort was evaluated in different scenarios where feasible mitigation strategies (replacement of materiality, addition of vegetation and sun shading elements) were applied to classify them according to their effectiveness using the ENVI-met simulation tool.

This research is structured as follows: the materials and methods used in the experimentation are detailed in Section 2. The results in terms of PMV and PPD of the current and the simulated scenarios are shown in Section 3 and they are discussed in Section 4. Finally, the conclusions obtained throughout the development of this research are presented in Section 5.

2. Materials and methods

2.1. Study area

This research was conducted in a pedestrian canyon street in the historic city centre of Huelva, located in the southwest of Spain (6°56′24″O, 37°15′58″N). Huelva is in the CSA climatic zone according to Köppen-Geiger climate classification [53]. Its climate is typical Subtropical-Mediterranean with Atlantic influences. In general, it has mild, windy and partly cloudy winters (with temperatures rarely falling below 5 °C), and hot, dry and clear summers (the warmest months are July and August when temperatures can occasionally exceed 40 °C). The annual average temperature is 18.2 °C, the annual average humidity is 66 %, and the annual average rainfall is 525 mm [54].

The analysed space in Santa Fe Street (Fig. 1) has an area of 1000 m^2 (50 m long × 20 m wide) and is for pedestrian use. It has an asymmetrical urban canyon configuration with the canyon's axys parallel to the N-S orientation and an aspect ratio of 1, i.e with a wide opening to the sky and including central and lateral rows of trees. It is bounded by a 2-storey building to the west and a 5-storey building to the east, both of which are for public use. To the north it is delimited by an asphalt road while to the south the pedestrian street continues for further metres. Regarding the materiality of the public space, the building façades are coated with brick tiles and ceramic blocks. The paving of the street is covered with red brick tiles. As for the vegetation, there are two tree species in the street: 3-metre high fruit trees next to the east and west facades and 8-metre high palm trees distributed in two strips on the centre of the street. The urban furniture consists of benches and litter bins located between the palm trees. In this way, the urban configuration created by the vegetation and furniture generates three pedestrian paths with N-S orientation: one in the west, one in the centre and one in the east.

2.2. Data acquisition and post-processing: In situ and aerial measurement

Data acquisition was carried out on 20 July 2021. Measurements were taken at different times of the day in order to analyse the variation of thermal comfort during a typical summer day. For this reason, three time periods were chosen with solar exposure during the morning and afternoon (11:00 h, 15:00 h, 19:00 h). Data was acquired at different points of the three N-S oriented trajectories identified in the urban canyon in order to estimate the urban thermal comfort in each of them.

Fig. 1. Santa Fe Street. 3D Model of RGB imagery from UAV.

A total of 12 points were chosen, 4 in each trajectory, with the aim of analysing all possible routes that a pedestrian can take when walking along Santa Fe Street. The data acquisition was carried out in two parts, an in situ and an aerial survey, which were performed at the same time by a team of two people.

The in-situ inspection consisted on the direct measurement of several environmental parameters that directly affect the two comfort indices analysed (PMV and PPD): air temperature, relative humidity and wind speed. A RS-91 Pro thermo-hygrometer (RS Components™, Corby, United Kingdom) was used to measure air temperature and relative humidity. It is a sensor capable of measuring air temperature in the range of 20.0 °C–60.0 °C with a measurement resolution of 0.1 °C, and relative humidity in the range of 0.0 % ~ 100.0 % with a measurement resolution of 0.1 %. The average air temperature recorded was 24.5 °C at 11:00 h, 30.4 °C at 15:00 h and 26.4 °C at 19:00 h. The average relative humidity recorded was 62.0 % at 11:00 h, 49.8 % at 15:00 h and 61.0 % at 19:00 h. During the inspection, the weather conditions were ideal in the early morning, a day with light cloud cover and little wind which progressively increased during the day (1.8 m/s at 11:00 h, 4.5 m/s at 15:00 h and 6.6 m/s at 19:00 h). Wind speed and direction data were obtained from the nearest weather station, located 2.5 km in a straight line from the case study. Like all weather stations of the Spanish State Meteorological Agency (AEMET), wind speed and direction are measured in a range between 2 and 10 m above ground level.

The aerial inspection consisted of acquiring the surface temperature of the pavement and façades for the estimation of another determining environmental factor in the calculation of both indices: the mean radiant temperature. For this purpose, an UAV equipped with a radiometric thermal camera was used to measure pixel temperature of thermal images. It is the DJI Mavic 2 Enterprise Advanced (DJI™, Nanshan, Shenzhen, China), a light drone that can reach a maximum speed of 72 km/h and a flight range of 31 min. It is equipped with two cameras, a RGB camera and a thermographic camera operating in the 8–14 µm spectral band. Both cameras work at the same time capturing visual, thermal or view-split images. The resolution of the thermographic sensor is high – 640x512 pixels - which allows flights over long

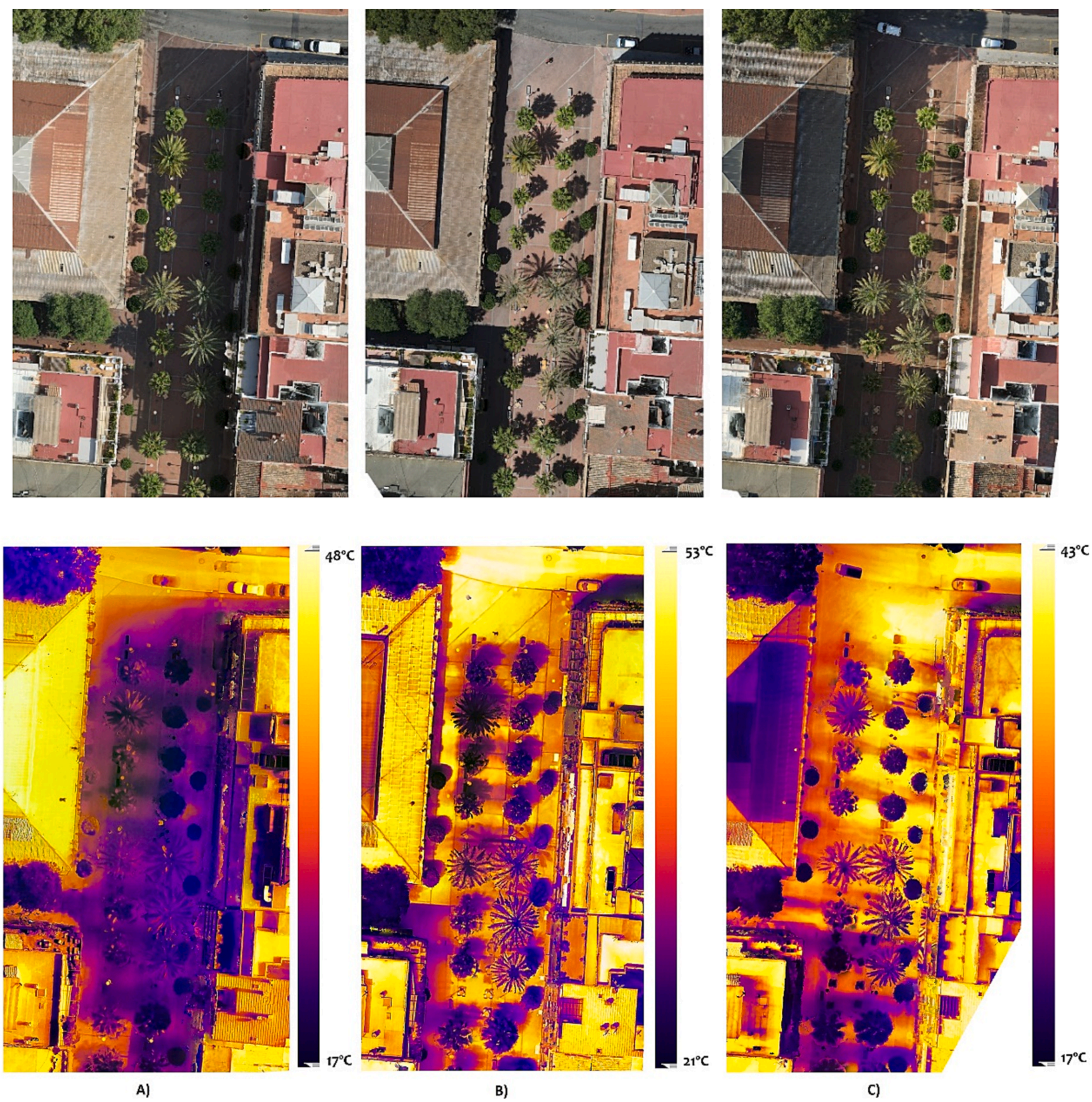

Fig. 2. Orthophotos of RGB and thermal imagery from UAV. A) At 11:00 h, B) At 15:00 h, C) At 19:00.

distances while keeping the accuracy of the measurements. The versatility of this tool made it possible to obtain multiple thermal data from different perspectives in the shortest possible time. A parachute of 40 g was attached for safety reasons when flying over an urban public space (to reduce the kinetic energy of impact in <80 J in the event of an accident). DJI Pilot™ software was used for flight execution and DJI Terra™ and DJI Thermal Analysis Tool™ were used for image post-processing.

DJI Pilot™ enables to draw, based on a satellite image, the way-points followed by the aircraft during the flight and to execute it automatically. In each time period analysed two flights were planned: one at +80 m altitude with a nadir perspective (90°) to post-process an orthophoto and with an oblique perspective (60°) to post-process a three-dimensional model of the street, and another at +3 m with an angle of 0° to capture individual images of the façades that delimit the urban canyon. Both flights took 25 min, requiring one battery. In total 1276 images were obtained from the UAV (638 thermal images and 638 RGB images) which were post-processed to obtain a three-dimensional model (Fig. 1) and orthophotos (Fig. 2) with DJI Terra™ software. This software allows creating and editing point clouds to generate high-precision 2D maps and 3D models based on aerial images. These processes are performed automatically thanks to its CPU core based on photogrammetry techniques and artificial vision algorithms.

Finally, the DJI Thermal Analysis Tools™ software was used to extract the surface temperatures from the thermal images and calculate the mean radiant temperature at each analysis point based on them. This software allows the image to be thermally compensated by introducing environmental parameters to obtain real surface temperature values for each pixel. Data related to the distance to the object at the time of capture, the emissivity of the material and the air temperature obtained in situ were also entered. Once the surface temperatures of the pavements and façades around the different points of analysis were extracted, solar radiation data was obtained from the nearest weather station to complete the calculation of the mean radiant temperature.

2.3. Calculation of urban thermal discomfort in the current scenario

The current thermal comfort of the urban canyon was evaluated by means of PMV and PPD terms. PMV is a thermal index developed by Fanger [4] who proposed an equation based on 1565 questionnaires related to the feeling of thermal comfort in an indoor space in order to evaluate its thermohygrometric qualities. Afterwards, it was adapted to outdoor spaces by parametrising short and long wave radiative fluxes [9]. The use of this index is suggested by the German engineering guidelines VDI 3787 [55], developed for outdoor environments and by the ISO 7730 [56] and the ASHRAE 55 [57], designed for indoor environments.

The PMV index predicts the mean value of the thermal sensation votes of a group of people. This equation is derived from the thermal equilibrium equation and depends on 6 parameters that influence thermal comfort: two human variables (clothing insulation and human activity) and four environmental variables (air temperature, relative air humidity, air velocity and mean radiant temperature). PMV was calculated following the equation (1) [58]:

$$PMV = \left[0.303 \cdot e^{-0,036M} + 0.028\right] \cdot L \tag{1}$$

where M is the rate of metabolic heat production (W/m^2) and L is the thermal load on the body, defined as the difference between internal heat production and heat loss to the environment:

where W is the rate of mechanical work accomplished (W/m2), fcl is the clothing area factor (dimensionless), tcl is the clothing temperature (°C), tr is the mean radiant temperature (°C), hc is the convective heat transfer coefficient (W/m2/°C), ta is the air temperature (°C) and pa is the partial water vapour pressure in air (kPa).

Following the equation (2), the metabolic rate M was supposed to be 100 W/m^2 corresponding to walking or leisurely strolling [55]. The rate of mechanical work W was estimated at 0 W/m^2. The clothing area factor fcl depends on the insulation of clothing Icl, which was chosen 0.5 clo corresponding to light summer clothing [59]. The clothing temperature was calculated by iteration following the equation (3) [11]:

$$tcl = 35.7 - 0.028\,(M - W) - Icl\left\{39.6 \cdot 10^{-9}\, fcl\,\left[(tcl + 273)^4 - (tr + 273)^4\right] + fcl\ hc\,(tcl - ta)\right\} \tag{3}$$

The mean radiant temperature tr is a key variable that simplifies radiant heat transfer in making thermal calculations for the human body. It includes both shortwave and longwave radiant heat exchange between the human body and the environment [60]. Fanger and Jendritzky et al. compiled an equation (4) for the calculation of tr [4,9]:

$$tr = \sqrt[4]{\frac{1}{\sigma}\sum_{i=1}^{n}\left(Ei + \alpha k\,\frac{Di}{\varepsilon p}\right)Fi + \frac{fp\ \alpha k\ I}{\varepsilon p\ \sigma}} \tag{4}$$

where σ is the Stephan-Boltzman constant (5.67 · 10^{-8} W/(m^{2}K^4), E is the longwave radiation, D is the shortwave radiation, F is the weight factor, αk is the absorption coefficient for short-wave radiation, εp is the emissivity of human skin, fp is the surface projection factor and I is the direct solar radiation. Shortwave radiation D was calculated from solar data acquired in situ while longwave radiation E was calculated using surface temperatures of facades and pavements acquired by aerial thermography [61].

The convective heat transfer coefficient is affected by wind velocity v and it was solved by iteration following the equation (5) [62]:

$$hc = 2.38\ |tcl - ta|^{0.25} for\ 2.38\ |tcl - ta|^{0.25} > 12.1\ \sqrt{v} \tag{5}$$

or,

$$hc = 12.1\ \sqrt{v}\ for\ 2.38\ |tcl - ta|^{0.25} < 12.1\ \sqrt{v}$$

The partial water vapour pressure in air pa is the product of saturated vapour pressure $psat$, the air temperature ta and the relative humidity RH [63]. Given the air temperature ta, the saturated vapour pressure $psat$ can be calculated using Antoine's formula.

PMV is represented on a 7- point scale with −3 representing "cold" and +3 representing "hot". Point 0 is considered to be a neutral thermal sensation, which is normally associated with a state of comfort. The seven-point scale follows: −3 = cold, −2 = cool, −1 = slightly cool, 0 = neutral, 1 = slightly warm, 2 = warm, and 3 = hot. Because PMV depends on the local climate, the set range can be exceeded. In fact, some research focused in outdoors extends the range between +4 and −4, being +4 (very hot) and −4 (very cold) [10].

From PMV, the PPD index representing the predicted percentage of people dissatisfied at each PMV can be calculated. PPD can be derived from PMV/thermal sensation votes as shown in equation (6) according to ISO7730 [56]:

$$PPD = 100 - 95 \cdot\ e^{-0.03353 \cdot PMV^4 + 0.2179 \cdot PMV^2} \tag{6}$$

All the results discussed below were calculated for a height of 1.2 m

$$M - W = 3.96 \cdot 10^{-8}\ fcl\ \left[(tcl + 273)^4 - (tr + 273)^4\right] + fcl\ hc(tcl - ta) + 3.05[5.73 - 0.007(M - W) - pa] + 0.42[(M - W) - 58.15] + 0.0173M(5.87 - pa) + 0.0014M(34 - ta) \tag{2}$$

above the ground. This height is representative for comfort calculations for a standing person. In the literature review, PMV and PPD indices showed a high correlation with actual thermal sensation votes derived from outdoor comfort surveys [64,65].

2.4. Simulation of urban thermal discomfort in various scenarios following different mitigation proposals

Once the thermal discomfort was quantified in different time periods of the current scenario, several mitigation proposals were studied by changing the design of the public space through computer simulation. The free late version of the ENVI-met software [66], which is specialised in the analysis of the effects of climatology, architecture and urban planning in cities, was used for this purpose. This tool allows the creation of microclimatic models based on the fundamental laws of fluid dynamics and thermodynamics and simulates the interactions between the surface, plants and the atmosphere in urban environments. ENVI-met simulates the microclimatic dynamics within a daily cycle in complex urban structures and its high spatial and temporal resolution allows a fine-grained understanding of the microclimate at street level. It requires relatively few input parameters and generates three-dimensional models and calculates all important meteorological factors such as air temperature, relative humidity, wind flows, turbulence, solar radiation fluxes, mean radiant temperature, etc. with a high spatial resolution (between 0.5 and 5 m horizontally) and temporal resolution (up to 5 s).

For the simulations, ENVI-met requires two main input files: the area input file defining the project location parameters and the urban space layout (building types, vegetation and soil); and the configuration file containing the simulation settings related to the meteorological parameters. Then, several areas input files were created with different layouts of the urban space and a configuration file with the meteorological parameters measured in situ (air temperature, relative humidity, wind speed and wind direction), which were combined to calculate the thermal discomfort indices PMV and PPD in new scenarios.

For all area input files, the study area was entered as a domain of 30 × 30 × 10 cells of 2 × 2 × 2 m each and the location was set to Huelva (Spain). For the buildings, the façade and roof material were set as default (moderately insulated). The different distributions of urban space applied viable thermal discomfort mitigation strategies and were presented as scenarios. In scenario 1 (S1) a change in the paving of Santa Fe street and the northern road was proposed. The red bricks tiles in the pedestrian zone were replaced with stone bricks in combination with grass and the asphalt of the road was replaced with concrete. In scenario 2 (S2) the vegetation was modified by doubling the number of trees (fruit trees and palm trees) following the existing rows of trees. In scenario 3 (S3) a new structure was included in the centre of the street, a 5 m high vegetation-covered pergola between the palm trees. Finally, in scenario 4 (S4) all the measures contemplated in scenarios 1, 2 and 3 were included. In the configuration file, the option simple forcing was chosen for the meteorological boundary condition. The simulation was carried out by combining the configuration file with the area input files and the output intervals of the files were adjusted every 60 min in the three-time sets studied (11:00 h, 15:00 h and 19:00 h).

Once the simulations were carried out, values of the new environmental variables were obtained at each of the analysis points and the two comfort indices were recalculated in the new scenarios to compare the results with the indices previously obtained in the current scenario S0. The ENVI-met software has been used as a comparative and validation method in previous studies on urban thermal comfort [61].

3. Results

According to the methodology described, the results obtained are shown below. The first section analyses urban thermal discomfort in the current scenario at different times (11:00 h, 15:00 h, 19:00 h) on a typical summer day. In the second section, several scenarios are analysed with different proposals for mitigating thermal discomfort in the most unfavourable time slot (15:00 h). The third section analyses the highest impact thermal discomfort mitigation scenario on the rest of the time slots (11:00 h, 19:00 h).

3.1. Analysis of current urban thermal discomfort (scenario 0) on a typical summer day

PMV and PPD indices were calculated in a matrix of 12 points distributed along the urban space. The matrix follows three possible pedestrian paths, according to the distribution of vegetation and urban furniture: *1* on the western side, *2* in the centre and *3* on the eastern side. Each line was subdivided into 4 points *A*, *B*, *C* and *D* (*A* being the point to the north and *D* the point to the south). Fig. 3 shows the location of the analysis points.

As Fig. 4 indicates, trajectory *1* proved to be more comfortable in the 19:00 h period (just when it is shaded by the western building) with PMV values around +0.2 and +0.5, corresponding to a neutral thermal sensation of the pedestrian, and a PPD index between 6 and 11.1%. However, during the morning (11:00 h), *1* is the only trajectory affected by the sun, and PMV values between +0.8 and +1.5 (slightly warm thermal sensation), and a PPD index between 19.1 and 52.3% were reached with great variability between the points along this path. At that time, *1A* was the most unfavourable point and the central points *1B* and *1C* were the most favourable. At 15:00 h, uncomfortable PMV values between +2.0 and +3.0, were on the boundary between warm and hot thermal sensitivity, and a PPD index around 77.3–99.9% were obtained.

Trajectory *2* at a central location on the street showed to be very comfortable in the morning (11:00 h) and in the evening (19:00 h) with PMV values close to +0.0, that means a neutral thermal sensation (at 11:00 h between +0 and +0.2, and at 19:00 h between +0.2 and +0.5), with a PPD index below 10% (at 11:00 h between 5.0 and 6.2%, and at 19:00 h between 5.6 and 9.8%). However, at 15:00 h PMV values were very close to the upper limit +3.0 (hot thermal sensitivity). A PPD index of 99% were observed at all four analysis points.

Trajectory *3* proved to be the most comfortable in the morning period (11:00 h), when it is shaded by the eastern building, with PMV values close to +0.0 (neutral thermal sensation) and a PPD index below 5%. During the afternoon (19:00 h), it is the only section affected by the sun. PMV values between +0.4 and +1.1 (neutral and slightly warm thermal sensation) and a PPD index between 8.1 and 31.1% were obtained, with *3A* being the most unfavourable point and *3D* the most favourable. At 15:00 h, uncomfortable PMV values between +2.4 and +3.0 (hot thermal sensitivity) and a PPD index above 90% (91.2–99.3%) were obtained.

Once PMV and PPD were calculated in situ in the current scenario (scenario 0), and prior to the simulation of these indices in the new scenarios in the most unfavourable time slot (15:00 h), the calculated and simulated indices were compared in scenario 0. For this purpose, two statistical metrics were used: the coefficient of determination (R^2) and the root mean square error (RMSE) [67]. R^2 describes the proportion of the total variance explained by the model, i.e., it is a measure of the goodness of fit or reliability of the estimated model to the data. The root mean square error (RMSE) is the standard deviation of the residuals (prediction errors). Residuals are a measure of the distance between the data points and the regression line. The RMSE indicates the total model error.

Fig. 5 shows the linear relationship between the calculated and simulated PMV and PPD values. The results demonstrated a strong coefficient of determination between the analysed values ($R^2 = 0.884$ in the PMV calculation and $R^2 = 0.827$ in the PPD calculation). The RMSE was 0.2 for PMV data (6.4 % error) and 2.9 for PPD data (3.1% error).

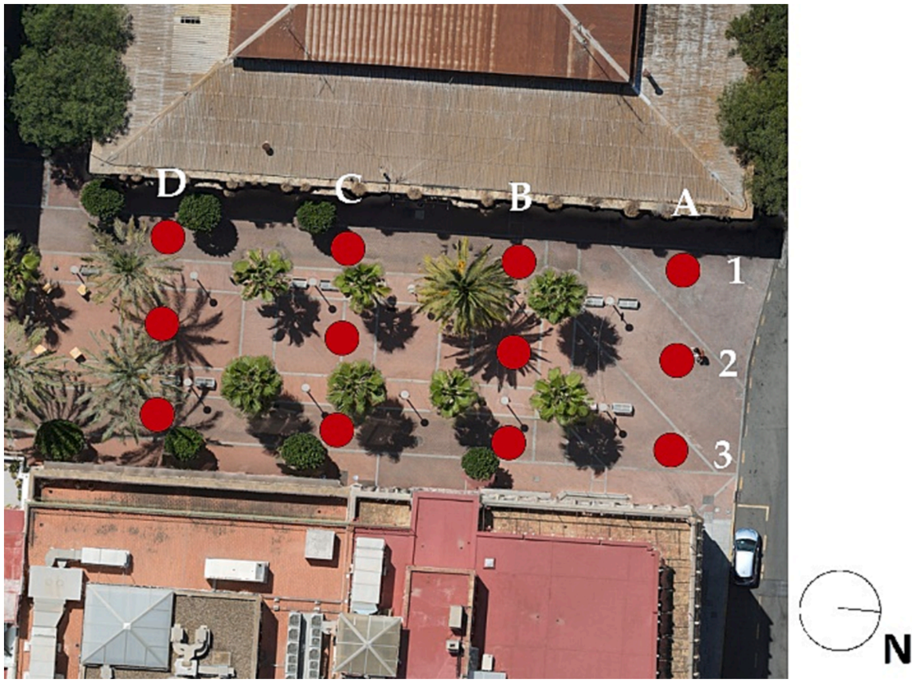

Fig. 3. Orthophoto of RGB imagery from UAV with thermal comfort measurement points.

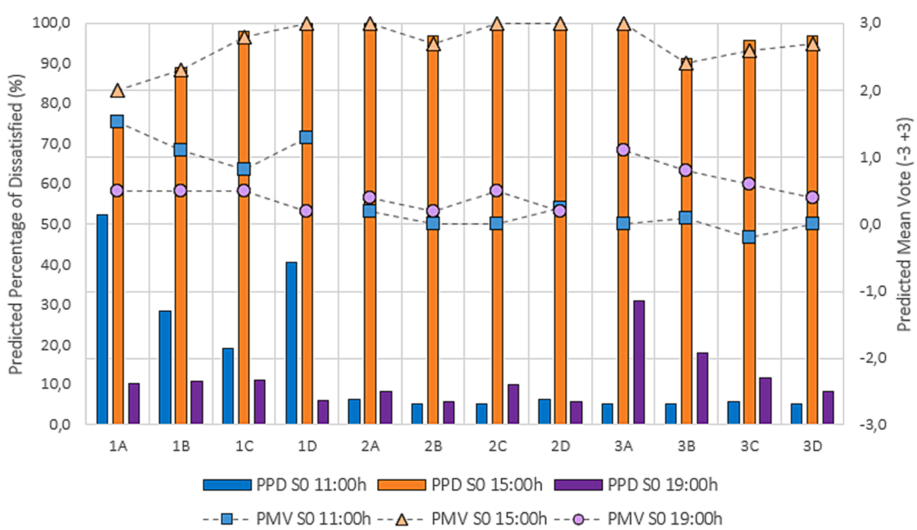

Fig. 4. Analysis of current urban thermal discomfort (Scenario 0) in PMV and PPD terms on a typical summer day.

3.2. Analysis of the influence of the thermal discomfort mitigation scenarios (scenarios 1–4) in the most unfavourable time slot (15:00 h)

In this section, thermal discomfort indices were calculated following the 12 points of the 3 trajectories in 4 scenarios simulated at 15:00 h. As previously mentioned, scenario 0 (S0) is the current scenario and it was used as a reference. In scenario 1 (S1) the pavements were replaced. In scenario 2 (S2) the existing vegetation was doubled on the sides of the street. In scenario 3 (S3) a vegetal pergola was added in the central area. Finally, in scenario 4 (S4) all the measures of the previous scenarios were included.

As Fig. 6 indicates, in the current scenario (S0) for trajectory *1*, a predicted mean vote (PMV) of about +2.5 (warm-hot thermal sensitivity) was obtained with a percentage of dissatisfied people (PPD) of about 91.0%. Analysing the mitigation measures in individual scenarios (S1, S2 and S3), the best performing scenario was S2, with a PMV of +1.5 and a PPD around 50.9%.

Regarding scenarios S1 and S3; S1 was most effective at the point near road *1A* (PMV: +1.6, PPD: 54.9%) while S3 had a slightly higher impact at the central points *1B*, *1C* and *1D* (PMV: +1.8, PPD: 65.8%). Scenario 4 (S4), which includes all mitigation measures, demonstrated a reduction in thermal discomfort with PMV values between +1.1 and +1.4 (slightly warm thermal sensation) and a PPD index of 28.4–43.3%, with point *1A* having the greatest thermal sensation.

For trajectory *2*, the current scenario (S0) showed a predicted mean vote (PMV) of +2.9 (hot thermal sensation), with a percentage of dissatisfied people (PPD) of 99.0% in the four analysis points. Analysing the mitigation measures separately (S1, S2 and S3), the scenario that provided the highest comfort was S3 with a PMV of +1.6 and a PPD of around 57.0%.

Regarding scenarios S1 and S2; S2 showed more comfortable results in all analysis points (PMV: +1.7, PPD: 59.9%) than S1 with PMV values

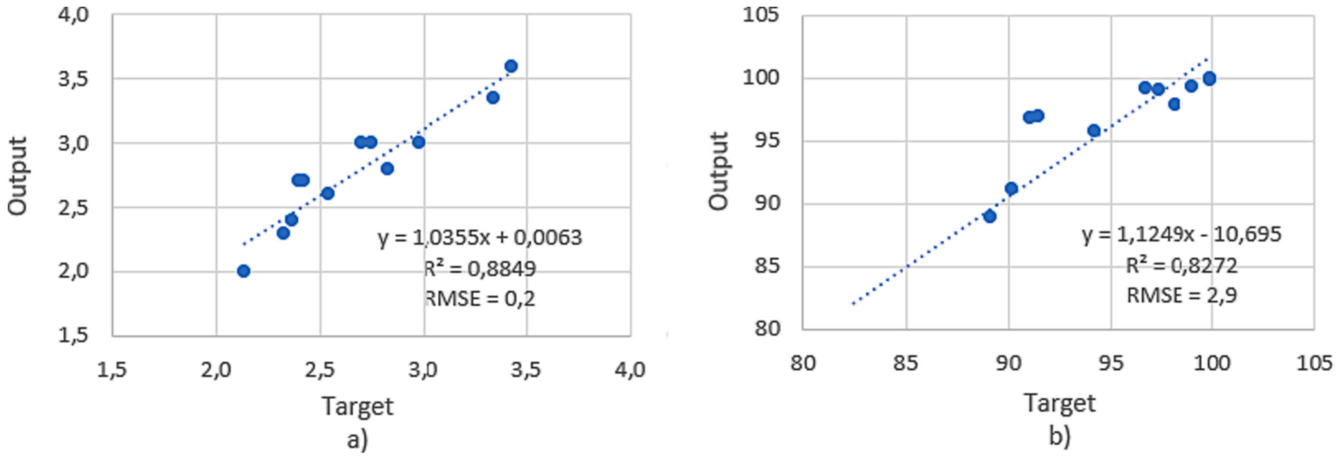

Fig. 5. Comparison of PMV and PPD calculated vs simulated in scenario 0 (R^2 and RMSE): a) PMV, b) PPD.

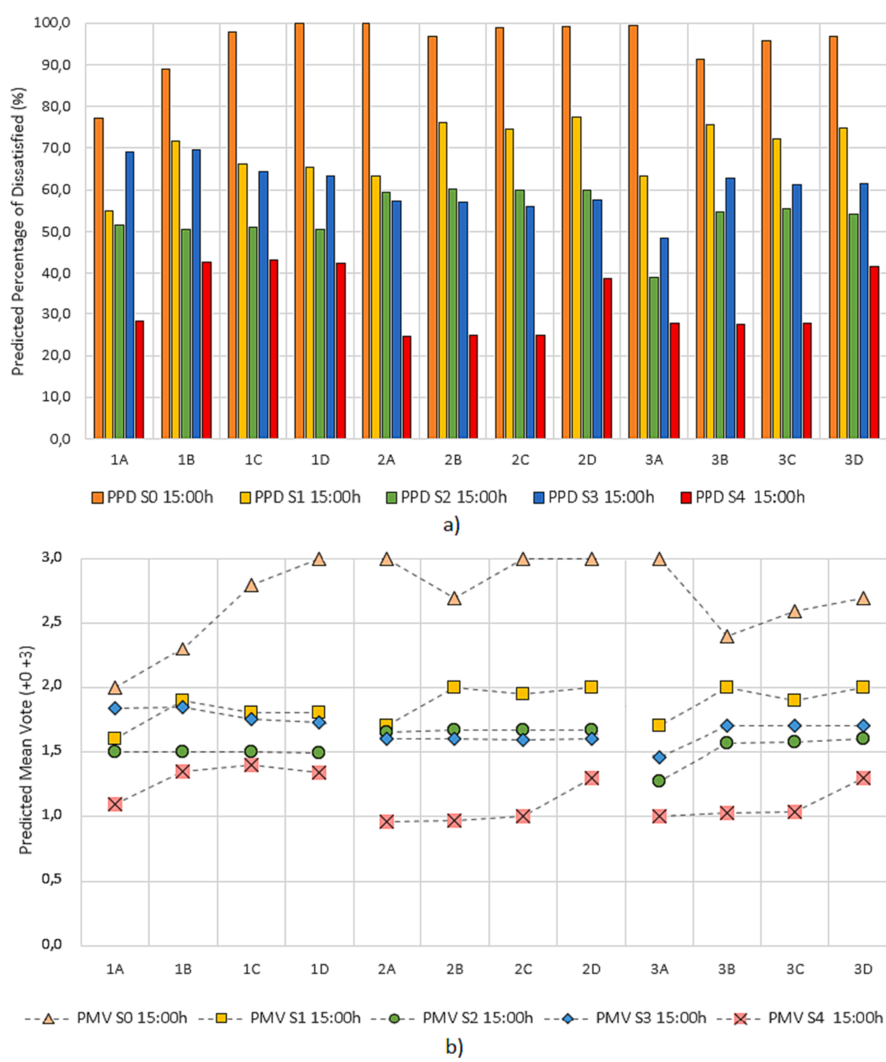

Fig. 6. Analysis of the influence of the thermal discomfort mitigation scenarios (Scenarios 1–4) in PMV and PPD terms in the most unfavourable time slot (15:00 h): a) PPD, b) PMV.

of +1.9 and PPD index over 72.9%, with *2A* being the most comfortable point in that scenario. Scenario 4 (S4), including all mitigation measures, showed an improvement in public comfort with PMV values around +1.0 and +1.3 (slightly warm thermal sensitivity) and a PPD index between 25 and 38.8%, with the most favourable points being *2A*, *2B* and *2C*.

Finally, trajectory *3* in the current scenario (S0), showed a predicted mean vote (PMV) of +2.7 (hot thermal sensation), with a percentage of dissatisfied people (PPD) of 95.8%. Analysing the mitigation measures individually (S1, S2 and S3), the best performing scenario was S2 with a PMV of +1.5 and a PPD around 50.8%, with *3A* being the most comfortable point.

Regarding scenarios S1 and S3; S3 showed more comfortable results in all analysis points (PMV: +1.6, PPD: 58.6%) than S1 with PMV values of +1.9 and a PPD index over 71.5%, with *3A* being the most favourable point in both scenarios. Scenario 4 (S4), which includes all mitigation measures, demonstrated a reduction in thermal discomfort with PMV values between +1.0 and +1.3 (slightly warm thermal sensitivity) and a PPD index of 27.4–41.7%, with the most favourable points being *3A*, *3B* and *3C*.

3.3. Analysis of the influence of the highest impact thermal discomfort mitigation scenario (scenario 4) on the rest of the day (11:00 h, 19:00 h)

In this section, thermal discomfort indices were calculated following the 12 points of the 3 trajectories in the simulated scenario with the highest mitigation impact in the remaining analysed hours of a typical summer day (11:00 h and 19:00 h). As previously mentioned, scenario 4 (S4) includes all the mitigation measures of the scenarios: pavement replacement, doubling of vegetation and addition of vegetated pergola.

During the morning (11.00 h), as shown in Fig. 7, scenario 4 gave counterproductive results as it was only effective in improving thermal comfort in trajectory *1*. In the current scenario (S0) for trajectory *1*, a predicted mean vote (PMV) of +1.2 (slightly warm thermal sensation), with a percentage of dissatisfied people (PPD) between 35.1% were obtained. S4 showed a reduction in thermal discomfort with PMV values between −0.3 and +0.0, which is translated in a neutral thermal sensation, and a PPD index between 5.0 and 6.7%. However, on the other trajectories, urban thermal discomfort was slightly increasing.

In S0, PMV values of trajectories *2* and *3* were about +0.1 and +0.0 (neutral thermal sensitivity) with PPD indices of 5.6% and of 5.2%, respectively. S4 showed a reduction in thermal comfort with PMV values between −0.1 and −0.3 for trajectory *2* and −0.1 and −0.4 for trajectory *3*, with PPD indices between 5.1 and 7.5% (2) and 5.2–7.7% (3).

During the evening (19:00 h), as shown in Fig. 8, the impact of scenario 4 resulted in an improvement of thermal comfort in all trajectories. In S0, a predicted mean vote (PMV) of +0.4 (neutral thermal sensation), with a percentage of dissatisfied people (PPD) between 9.5% were obtained for trajectory *1*. S4 showed a reduction in thermal discomfort with PMV values around −0.2 and a PPD index of 5.6%.

For trajectory *2* that resulted in +0.3 for PMV and 7.3% for PPD in S0, the thermal comfort improved slightly with a PMV value around −0.3 and a PPD index of 6.2% in S4. In this trajectory, except for point *2C* which improved the feeling of comfort and decreased the percentage of dissatisfied people, the rest of points *2A*, *2B* and *2D* provided constant values of thermal comfort in both scenarios.

Finally, trajectory *3* in S0 showed a PMV value of +0.7 (between neutral and slightly warm thermal sensation) with a PPD index of 17.2%. S4 resulted in an increase in thermal comfort with PMV values between −0.1 and −0.2 and a PPD index around 5.2–5.6%.

4. Discussion

According to the results analysed, the discussion of the findings is as follows. In the current scenario (S0), at 11:00 h and 19:00 h two of the three trajectories are shaded by buildings and showed that: i) they are neutrally comfortable with PMV values close to +0 and PPD below 10%; ii) the morning shaded trajectories are slightly more thermally comfortable than the afternoon shaded trajectories, while the afternoon sun-exposed trajectory is slightly more thermally comfortable than the morning sunny trajectory (in both cases with PMV values around +1 and PPD varying between 17 and 35%); and iii) the most unfavourable point on the sunny routes is the point closest to the asphalt road (with PPD values between 31 and 52%). At 15:00 h, all three trajectories are exposed to the sun and showed that none of them were comfortable with PMV values close to +3.0, which translates into an uncomfortably hot thermal sensation, and an average PPD above 90% in all trajectories: 91% (1), 99% (2) and 96% (3). Based on these results, the following paragraphs discusses which mitigation measures would be optimal to improve the pedestrian's sense of comfort on the street at 15:00 h.

Scenario 1 (S1), which proposes a replacement of the asphalt of the road with concrete and of the red brick tiles in the pedestrian zone with stone bricks in combination with grass, showed a percentage improvement in the PMV of 28.3% for trajectory *1*, 34.4% for trajectory *2* and 28.2% for trajectory *3* with respect to S0. The PPD index decreased compared to the original scenario by 28.8% (1), 26.2% (2) and 25.2% (3). This scenario substantially improved the feeling of comfort of the points close to the road (1A, 2A and 3A) but overall, it had the least improvement impact compared to the rest of scenarios. Scenario 2 (S2), which proposes doubling the number of palm and fruit trees, showed an improvement in the PMV of 39.1% for trajectory *1*, 43.0% for trajectory *2* and 43.1% for trajectory *3* compared to S0. The PPD index decreased compared to S0 by 43.5% (1), 39.4 (2) and 46.7% (3). Comparing S1, S2 and S3 individually, S2 had the greatest impact on improving comfort in lateral trajectories *1* and *3*. Scenario 3 (S3), which proposes to incorporate a 5-metre high vegetal pergola between the palm trees providing

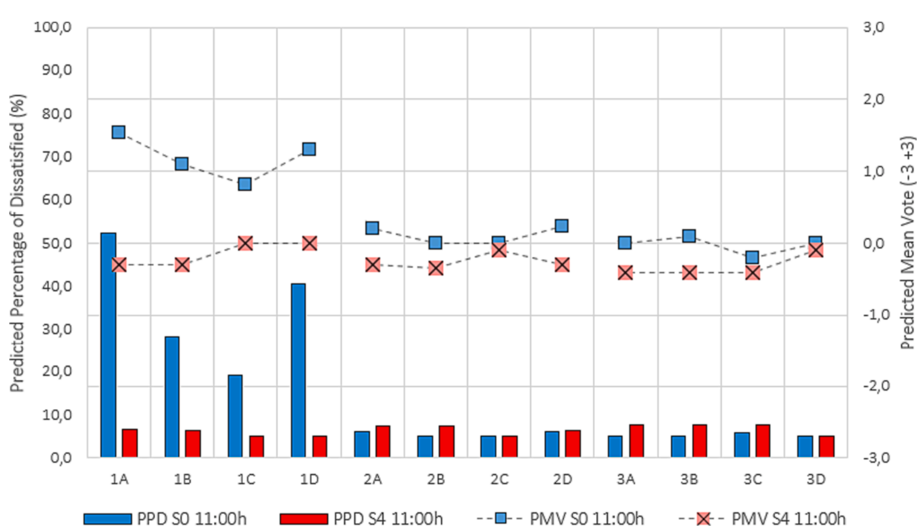

Fig. 7. Analysis of the influence of the thermal discomfort mitigation scenario S4 in PMV and PPD terms at 11:00 h.

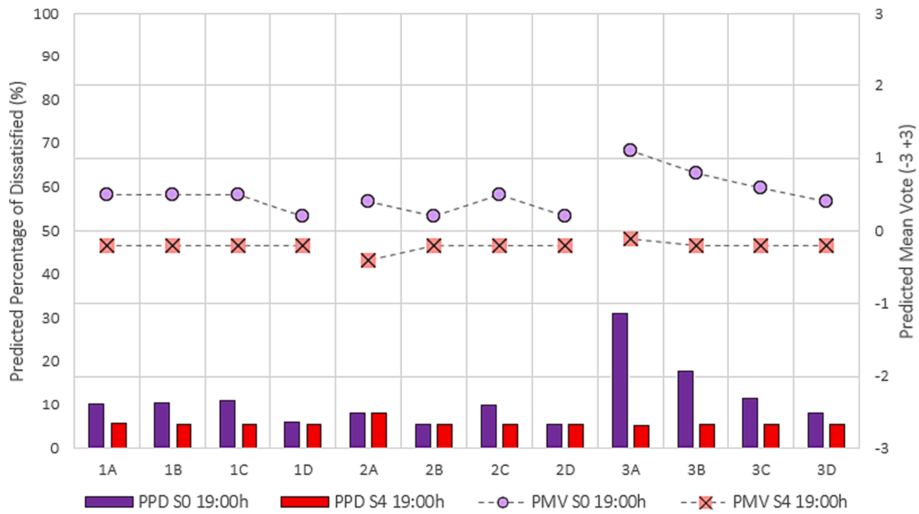

Fig. 8. Analysis of the influence of the thermal discomfort mitigation scenario S4 in PMV and PPD terms at 19:00 h.

shade over the central path of the street, showed a percentage improvement in the PMV of 26.8% for trajectory *1*, 45.3% for trajectory *2* and 38.0% for trajectory *3* with respect to S0. The PPD index decreased compared to S0 by 25.8% (1), 42.3 (2) and 38.6% (3). S3 had the greatest impact on improving comfort in the central trajectory *2*. However, it is remarkable that it was the only measure that did not show an equal improvement of the three trajectories and furthermore, compared to S2, it only showed a slight improvement in comfort in trajectory *2*.

Finally, S4 scenario - which includes all measures - gave the most comfortable results in all trajectories, with a percentage improvement in the PMV of 47.9% for trajectory *1*, 63.9% for trajectory *2* and 58.9% for trajectory *3* compared to scenario S0. The PPD index decreased compared to S0 by 57.2% (1), 71.3% (2) and 67.5% (3). Comparing all sub-points of analysis, the simulated PMV varied on a scale between +1.0 and +1.4 (generating a slightly warm generalised thermal sensation) while the PPD remained below 50% at any point along the street (24.6–43.3%).

Although comfortable results were obtained at 11:00 h and 19:00 h in the shaded and sunny trajectories, the S4 scenario was also applied at these times to analyse its impact. Remarkably, S4 only showed an improvement in thermal comfort on the sunny trajectory and slightly impaired it on the shady trajectories at 11:00 h. Compared to S0, S4 showed a PMV improvement of 88.3% and a PPD reduction of 81.5% for sunny trajectory *1*. However, the simulated scenario was counterproductive in the shaded areas (*2* and *3*) although with a marginal impact. The average PMV value varied slightly from +0.0 in S0 to −0.3 in S4 and the same trend was observed in the average PPD value which increased from 5.4% to 6.8%. At 19:00 h, the trend of S4 was also favourable for the sunny trajectory. Compared to S0, S4 showed a PMV improvement percentage of 70.6% and a PPD reduction of 58.8% for the sunny trajectory *3*. Contrary to 11:00 h, several points in the shaded trajectories (*2* and *3*) maintained constant or slightly improved thermal comfort in the new scenario. The average value of PMV varied slightly from +0.4 in S0 to −0.2 in S4 and PPD decreased from 8.4% to 5.9%.

It is important to say that there is a limitation in this research regarding to the proposition of mitigation measures, which are focused on the rehabilitation of the public space and not on its complete renovation. Therefore, since the vegetation is increased on the sides of the street following the existing row of trees and the pergola is introduced in the central part, it is reasonable to assume that the scenario including the vegetation (S2) is more effective on the side paths and the scenario including the pergola (S3) is more effective on the central path. In future researches, it would be interesting to examine how the inclusion of a vegetated pergola covering the width of the street, and therefore all trajectories, would affect S3. As well as, in S2, the addition of more vegetation, especially in the central part. Regarding S1, the inclusion of other surfaces such as water surfaces or cold pavements [68], that include high solar reflectance in their composition with the use of reflective aggregates or in their termination with a reflective surface coating, could be considered.

5. Conclusions

This work aims to contribute to a better understanding of the summer thermal sensation of urban canyons typical of subtropical cities. It is important to achieve climate-friendly urban design in order to ensure acceptable urban thermal comfort, especially in over-urbanised city centres during summer periods. In this research, an urban canyon located in the historical centre of the subtropical city of Huelva (Spain) was analysed. After a survey carried out by in situ meteorological sensors and airborne infrared sensors (equipped on a UAV), the current thermal comfort was analysed in terms of PMV and PPD at different times of the day (11:00 h, 15:00 h and 19:00 h) with the aim of formulating design recommendations for the rehabilitation of the urban canyon.

The results showed that the most thermally comfortable urban canyon routes corresponded to those that were shaded by buildings (at 11:00 h and 19.00 h). However, the results showed that the sunny trajectories (in the morning and afternoon hours) were just moderately uncomfortable with a slightly warm thermal sensation. The most unfavourable points were located next to the road due to the influence of road traffic. The main problem occurred in the early afternoon, at 15:00 h, when all paths are exposed to the sun and the percentage of dissatisfied people was higher than 90% at any point of the urban canyon showing that even activities requiring a low metabolic rate such as walking or leisurely strolling are incompatible on summer conditions in subtropical cities.

Given the importance of solar influence, shading is one of the most effective strategies to mitigate summer heat stress in cities with a subtropical climate. It is important to mention that the results obtained are based on an urban canyon configuration with aspect ratio = 1 and N-S orientation. At these latitudes, it is recommended to avoid W-E orientations as N-S orientations guarantee morning and afternoon shading on at least one side of the urban canyon. In these cases, the central hours of the day are the most detrimental to a comfortable environment.

To improve thermal discomfort at the most unfavourable time (15:00 h), different mitigation measures (replacement of materiality, addition of vegetation and sun shading elements) were proposed using the ENVI-met simulation tool. Overall, scenario 1 with the replacement of pavements improved the PMV value by 30% and decreased the PPD value by about 27%. Scenario 2, with the doubling of vegetation, improved the PMV value by 42% and decreased the PPD value by about 43%. Scenario 3, with the addition of the central pergola, improved the PMV value by 37% and decreased the PPD value by about 36%.

Comparing the proposed mitigation measures, shading strategies such as rows of trees or galleries proved to be effective for the design rehabilitation of this type of urban canyon. Several rows of vegetation around the centre and sides of the canyon were more effective than a single central gallery. The degree to which vegetation is effective in reducing thermal discomfort depends on its density (LAI) and the size of the tree. Typically, trees with lower foliage density provide less shade but more air circulation around them. In this research, two types of trees have been analysed: palm trees and fruit trees, characteristic of subtropical and Mediterranean cities.

Applying all the proposed measures in a single scenario, scenario 4, the best results were obtained in general terms, with a substantial improvement of 57% in the PMV value (with values around +1 that translate into a slightly warm thermal sensation) and a 65% decrease in the percentage of dissatisfied people (PPD) in all points of the urban canyon at the most unfavourable time of the day (15:00 h). However, the application of the measures in the remaining hours analysed that already offered a pleasant thermal comfort situation in the current scenario (11:00 h and 19:00 h) resulted in a significant improvement of the PMV and PPD values in the sunny trajectories but their impact was null or counterproductive (slightly worsening the thermal comfort) in the shaded trajectories. The conclusion is that shading strategies are necessary in the central hours of the day, but their effect on shaded spaces in the morning and afternoon was marginal.

It is necessary to mention that the effectiveness of shading strategies depends on the orientation and vertical proportion of the urban canyon. With this study, it is intended to contribute to a more complete overview in the analysis of the microclimate of urban canyons. The results presented can be of great use to the scientific community and urban planning experts when rehabilitating urban spaces in use. In future research, it is intended to develop a generally applicable methodology for this type of study through other case studies in which more exhaustive experiments are carried out by measuring in situ more variables that directly affect thermal comfort and validating the methodology in situ using alternatives to simulation.

Author contributions

M.V.R., conceived the idea, carried out the experimentation, wrote the article and made the corrections and revision; S.G.M., conceived the idea, carried out the experimentation and checked the manuscript; J.M. A.M., supervised and reviewed all work and the manuscript. All authors have read and agreed to the published version of the manuscript.

Funding

This work has been funded by the Research Center for Technology, Energy and Sustainability (CITES) at the University of Huelva.

This work has been also funded by Proyecto SALTES (P20_00730): Smartgrid with reconfigurable Ar- chitecture for testing controL Techniques and Energy Storage priority. Programa Operativo FEDER 2014-2020 Junta de Andalucia.

Funding for open access charge: Universidad de Huelva/CBUA.

Declaration of Competing Interest

The authors declare that they have no known competing financial interests or personal relationships that could have appeared to influence the work reported in this paper.

Data availability

Data will be made available on request.

References

[1] Y. Wang, U. Berardi, H. Akbari, Comparing the effects of urban heat island mitigation strategies for Toronto, Canada, Energ. Build. 114 (2016) 2–19, https://doi.org/10.1016/j.enbuild.2015.06.046.
[2] Á. Gulyás, J. Unger, A. Matzarakis, Assessment of the microclimatic and human comfort conditions in a complex urban environment: Modelling and measurements, Build. Environ. 41 (12) (2006) 1713–1722, https://doi.org/10.1016/j.buildenv.2005.07.001.
[3] M.C. Koppe, S. Kovats, B. Jendrizky, Health and global environmental change; heat-waves: risks and responses, series no.2, energy, environment and sustainable development, World Health Organization, Copenhagen, 2004.
[4] P.O. Fanger, Thermal Comfort: Analysis and Applications in Environmental Engineering, McGraw-Hil, New York, 1972.
[5] International Organisation for Standardisation, ISO 7730:1994 Moderate thermal environments: determination of PMV and PPD indices and specification of the conditions for thermal comfort. Geneva, Switzerland, 1994.
[6] P. Höppe, The physiological equivalent temperature - a universal index for the biometeorological assessment of the thermal environment, Int. J. Biometeorol. 43 (2) (1999) 71–75.
[7] J. Pickup and R. D. de Dear, An Outdoor Thermal Comfort Index (Out-Set*) -Part I –the Model and Its Assumptions, *15th ICB ICUC*, no. January 1999, pp. 1–7, 2000.
[8] G. Jendritzky, R. de Dear, G. Havenith, UTCI - why another thermal index ? Int. J. Biometeorol. 56 (3) (2012) 421–428.
[9] G. Jendritzky, W. Nübler, A model analysing the urban thermal environment in physiologically significant termsEin physiologisch relevarites Analysenmodell für die thermischen Bedingungen in der Stadtklimatologie, Arch. Meteorol. Geophys. Bioclimatol. Ser. B 29 (4) (1981) 313–326.
[10] F. Salata, I. Golasi, E. Vollaro, F. Bisegna, F. Nardecchia, M. Coppi, F. Gugliermetti, A. Vollaro, Evaluation of different urban microclimate mitigation strategies through a PMV analysis, Sustain. 7 (7) (2015) 9012–9030.
[11] N.H.M. Hashim, K.W. Tan, Y. Ling, Determination of thermal comfort for social impact assessment: Case study in Kota Damansara, Selangor, Malaysia, Am. J. Appl. Sci. 13 (11) (2016) 1156–1170, https://doi.org/10.3844/ajassp.2016.1156.1170.
[12] S. Sangkertadi, R. Syafriny, New equation for estimating outdoor thermal comfort in humid-tropical environment, Eur. J. Sustain. Dev. 3 (4) (2014) 43–52, https://doi.org/10.14207/ejsd.2014.v3n4p43.
[13] F. Canan, I. Golasi, V. Ciancio, M. Coppi, F. Salata, Outdoor thermal comfort conditions during summer in a cold semi-arid climate. A transversal field survey in Central Anatolia (Turkey), Build. Environ. 148 (2019) 212–224, https://doi.org/10.1016/j.buildenv.2018.11.008.
[14] J. Mi, B.o. Hong, T. Zhang, B. Huang, J. Niu, Outdoor thermal benchmarks and their application to climate-responsive designs of residential open spaces in a cold region of China, Build. Environ. 169 (2020) 106592.
[15] R. Abd Elraouf, A. Elmokadem, N. Megahed, O. Abo Eleinen, S. Eltarabily, The impact of urban geometry on outdoor thermal comfort in a hot-humid climate, Build. Environ. 225 (2022) 109632.
[16] F. Ali-Toudert, H. Mayer, Effects of asymmetry, galleries, overhanging façades and vegetation on thermal comfort in urban street canyons, Sol. Energy 81 (6) (2007) 742–754, https://doi.org/10.1016/j.solener.2006.10.007.
[17] F. Ali-Toudert, H. Mayer, Thermal comfort in an east-west oriented street canyon in Freiburg (Germany) under hot summer conditions, Theor. Appl. Climatol. 87 (1–4) (2007) 223–237, https://doi.org/10.1007/s00704-005-0194-4.
[18] F. Ali-Toudert, H. Mayer, Numerical study on the effects of aspect ratio and orientation of an urban street canyon on outdoor thermal comfort in hot and dry climate, Build. Environ. 41 (2) (2006) 94–108, https://doi.org/10.1016/j.buildenv.2005.01.013.
[19] E. Krüger, P. Drach, R. Emmanuel, O. Corbella, Assessment of daytime outdoor comfort levels in and outside the urban area of Glasgow, UK, Int. J. Biometeorol. 57 (4) (2013) 521–533, https://doi.org/10.1007/s00484-012-0578-y.
[20] J. Spagnolo, R. de Dear, A field study of thermal comfort in outdoor and semi-outdoor environments in subtropical Sydney Australia, Build. Environ. 38 (5) (2003) 721–738, https://doi.org/10.1016/S0360-1323(02)00209-3.
[21] M. Tsitoura, T. Tsoutsos, T. Daras, Evaluation of comfort conditions in urban open spaces. Application in the island of Crete, Energy Convers. Manag. 86 (2014) 250–258, https://doi.org/10.1016/j.enconman.2014.04.059.
[22] Z. Fang, Z. Lin, C.M. Mak, J. Niu, K.-T. Tse, Investigation into sensitivities of factors in outdoor thermal comfort indices, Build. Environ. 128 (2018) 129–142.
[23] K. Pantavou, M. Santamouris, D. Asimakopoulos, G. Theoharatos, Empirical calibration of thermal indices in an urban outdoor Mediterranean environment, Build. Environ. 80 (2014) 283–292, https://doi.org/10.1016/j.buildenv.2014.06.001.
[24] P. Bröde, E.L. Krüger, F.A. Rossi, D. Fiala, Predicting urban outdoor thermal comfort by the Universal Thermal Climate Index UTCI-a case study in Southern Brazil, Int. J. Biometeorol. 56 (3) (2012) 471–480, https://doi.org/10.1007/s00484-011-0452-3.
[25] F. Salata, I. Golasi, R. de Lieto Vollaro, A. de Lieto Vollaro, Outdoor thermal comfort in the Mediterranean area. A transversal study in Rome, Italy, Build. Environ. 96 (2016) 46–61, https://doi.org/10.1016/j.buildenv.2015.11.023.

[26] I. Golasi, F. Salata, E. de Lieto Vollaro, M. Coppi, A. de Lieto Vollaro, Thermal perception in the mediterranean area: Comparing the mediterranean outdoor comfort index (moci) to other outdoor thermal comfort indices, Energies 9 (7) (2016) pp, https://doi.org/10.3390/en9070550.
[27] S.P. Corgnati, M. Filippi, S. Viazzo, Perception of the thermal environment in high school and university classrooms: Subjective preferences and thermal comfort, Build. Environ. 42 (2) (2007) 951–959, https://doi.org/10.1016/j.buildenv.2005.10.027.
[28] C. Buratti, P. Ricciardi, Adaptive analysis of thermal comfort in university classrooms: Correlation between experimental data and mathematical models, Build. Environ. 44 (4) (2009) 674–687, https://doi.org/10.1016/j.buildenv.2008.06.001.
[29] S.P. Corgnati, R. Ansaldi, M. Filippi, Thermal comfort in Italian classrooms under free running conditions during mid seasons: Assessment through objective and subjective approaches, Build. Environ. 44 (4) (2009) 785–792, https://doi.org/10.1016/j.buildenv.2008.05.023.
[30] L. Dias Pereira, D. Raimondo, S.P. Corgnati, M. Gameiro da Silva, Assessment of indoor air quality and thermal comfort in Portuguese secondary classrooms: Methodology and results, Build. Environ. 81 (2014) 69–80, https://doi.org/10.1016/j.buildenv.2014.06.008.
[31] E. Johansson, S. Thorsson, R. Emmanuel, E. Krüger, Instruments and methods in outdoor thermal comfort studies - The need for standardization, Urban Clim. 10 (P2) (2014) 346–366, https://doi.org/10.1016/j.uclim.2013.12.002.
[32] F. Salata, I. Golasi, A.D.L. Vollaro, R.D.L. Vollaro, How high albedo and traditional buildings' materials and vegetation affect the quality of urban microclimate. A case study, Energ. Buildings 99 (2015) 32–49, https://doi.org/10.1016/j.enbuild.2015.04.010.
[33] F. Salata, I. Golasi, R. de Lieto Vollaro, A. de Lieto Vollaro, Urban microclimate and outdoor thermal comfort. A proper procedure to fit ENVI-met simulation outputs to experimental data, Sustain. Cities Soc. 26 (2016) 318–343.
[34] I. Karakounos, A. Dimoudi, S. Zoras, The influence of bioclimatic urban redevelopment on outdoor thermal comfort, Energ. Buildings 158 (2018) 1266–1274, https://doi.org/10.1016/j.enbuild.2017.11.035.
[35] S. Tsoka, A. Tsikaloudaki, T. Theodosiou, Analyzing the ENVI-met microclimate model's performance and assessing cool materials and urban vegetation applications–A review, Sustain. Cities Soc. 43 (2018) 55–76, https://doi.org/10.1016/j.scs.2018.08.009.
[36] R. Soares, H. Corvacho, F. Alves, Summer thermal conditions in outdoor public spaces: A case study in a mediterranean climate, *Sustain.*, 13 (10), 2021, doi: 10.3390/su13105348.
[37] R.A. Elraouf, A. ELMokadem, N. Megahed, O.A. Eleinen, S. Eltarabily, Evaluating urban outdoor thermal comfort: a validation of ENVI-met simulation through field measurement, J. Build. Perform. Simul. 15 (2) (2022) 268–286, https://doi.org/10.1080/19401493.2022.2046165.
[38] E. Andreou, Thermal comfort in outdoor spaces and urban canyon microclimate, Renew. Energy 55 (2013) 182–188, https://doi.org/10.1016/j.renene.2012.12.040.
[39] N. Abdollahzadeh, N. Biloria, Outdoor thermal comfort: Analyzing the impact of urban configurations on the thermal performance of street canyons in the humid subtropical climate of Sydney, Front. Archit. Res. 10 (2) (2021) 394–409, https://doi.org/10.1016/j.foar.2020.11.006.
[40] A. Yoshida, K. Tominaga, S. Watatani, Field measurements on energy balance of an urban canyon in the summer season, Energ. Build. 15 (3–4) (1990) 417–423, https://doi.org/10.1016/0378-7788(90)90016-C.
[41] X. Yang, L. Zhao, M. Bruse, Q. Meng, Evaluation of a microclimate model for predicting the thermal behavior of different ground surfaces, Build. Environ. 60 (2013) 93–104, https://doi.org/10.1016/j.buildenv.2012.11.008.
[42] M. Santamouris, N. Papanikolaou, I. Koronakis, I. Livada, D. Asimakopoulos, Thermal and air flow characteristics in a deep pedestrian canyon under hot weather conditions, Atmos. Environ. 33 (27) (1999) 4503–4521, https://doi.org/10.1016/S1352-2310(99)00187-9.
[43] R. Emmanuel, H. Rosenlund, E. Johansson, Urban shading - A design option for the tropics? A study in Colombo, Sri Lanka, Int. J. Climatol. 27 (14) (2007) 1995–2004, https://doi.org/10.1002/joc.1609.
[44] A. Matzarakis, H. Mayer, M.G. Iziomon, Applications of a universal thermal index: Physiological equivalent temperature, Int. J. Biometeorol. 43 (2) (1999) 76–84, https://doi.org/10.1007/s004840050119.
[45] E. Gatto *et al.*, Analysis of urban greening scenarios for improving outdoor thermal comfort in neighbourhoods of lecce (Southern Italy), *Climate*, 9 (7), 2021, doi: 10.3390/cli9070116.
[46] S. Yin, F. Wang, Y. Xiao, S. Xue, Comparing cooling efficiency of shading strategies for pedestrian thermal comfort in street canyons of traditional shophouse neighbourhoods in Guangzhou, China, Urban Clim. 43 (2022) 101165.
[47] E. Alexandri, P. Jones, Temperature decreases in an urban canyon due to green walls and green roofs in diverse climates, Build. Environ. 43 (4) (2008) 480–493, https://doi.org/10.1016/j.buildenv.2006.10.055.
[48] K. Perini, A. Magliocco, Effects of vegetation, urban density, building height, and atmospheric conditions on local temperatures and thermal comfort, Urban For. Urban Green. 13 (3) (2014) 495–506, https://doi.org/10.1016/j.ufug.2014.03.003.
[49] C. Georgakis, S. Zoras, M. Santamouris, Studying the effect of 'cool' coatings in street urban canyons and its potential as a heat island mitigation technique, Sustain. Cities Soc. 13 (2014) 20–31, https://doi.org/10.1016/j.scs.2014.04.002.
[50] F. Salata, I. Golasi, D. Petitti, E. de Lieto Vollaro, M. Coppi, A. de Lieto Vollaro, Relating microclimate, human thermal comfort and health during heat waves: An analysis of heat island mitigation strategies through a case study in an urban outdoor environment, Sustain. Cities Soc. 30 (2017) 79–96, https://doi.org/10.1016/j.scs.2017.01.006.
[51] D. Elgheznawy, S. Eltarabily, The impact of sun sail-shading strategy on the thermal comfort in school courtyards, Build. Environ. 202 (2021) 108046.
[52] M. Videras Rodríguez, S. G. Melgar, A. S. Cordero, and J. M. A. Márquez, A Critical review of unmanned aerial vehicles (UAVs) use in architecture and urbanism: scientometric and bibliometric analysis, *Appl. Sci.*, vol. 11, no. 21, p. 9966, Oct. 2021, doi: 10.3390/app11219966.
[53] M.C. Peel, B.L. Finlayson, T.A. McMahon, Updated world map of the Köppen-Geiger climate classification, Hydrol. Earth Syst. Sci. 11 (5) (2007) 1633–1644, https://doi.org/10.1002/ppp.421.
[54] Annual climatological values. Huelva, Ronda Este - Agencia Estatal de Meteorología (AEMET). Gobierno de España. http://www.aemet.es/es/serviciosclimaticos/datosclimatologicos/valoresclimatologicos?l=4642E&k=and (accessed Feb. 16, 2022).
[55] Verein Deutscher Ingenieure, VDI 3787 Environmental meteorology: Methods for the human biometeorological evaluation of climate and air quality for urban and regional planning at regional level; Part I: Climate, Beuth Verlag, Berlin, Germany, 2008.
[56] International Organisation for Standardisation, ISO 7730:2005 Ergonomics of the thermal environment: analytical determination and interpretation of thermal comfort using calculation of the PMV and PPD indices and local thermal comfort criteria. Geneva, Switzerland, 2005.
[57] American Society of Heating Refrigerating and Air-Conditioning Engineers, *ASHRAE Standard 55:2010 Thermal environmental conditions for human occupancy*. Atlanta, GA, USA, 2010.
[58] American Society of Heating Refrigerating and Air-Conditioning Engineers, *ASHRAE Handbook Fundamentals, Chapter 9: Thermal comfort*. Atlanta GA USA, 2009.
[59] Y.Y. Yan, J.E. Oliver, The clo : a utilitarian unit to measure weather/climate comfort, Int. J. Climatol. 16 (9) (1996) 1045–1056, https://doi.org/10.1002/(SICI)1097-0088(199609)16:9<1045::AID-JOC73>3.0.CO;2-O.
[60] H. Guo, D. Aviv, M. Loyola, E. Teitelbaum, N. Houchois, F. Meggers, On the understanding of the mean radiant temperature within both the indoor and outdoor environment, a critical review, *Renew. Sustain. Energy Rev.*, 117 (December) 2018, 109207, 2020, doi: 10.1016/j.rser.2019.06.014.
[61] M.V. Rodríguez, S.G. Melgar, J.M.A. Márquez, Assessment of aerial thermography as a method of in situ measurement of radiant heat transfer in urban public spaces, Sustain. Cities Soc. (October) (2022), 104228, https://doi.org/10.1016/j.scs.2022.104228.
[62] D. Enescu, A review of thermal comfort models and indicators for indoor environments, Renew. Sustain. Energy Rev. 79 (2017) 1353–1379, https://doi.org/10.1016/j.rser.2017.05.175.
[63] A.H. Harvey, P.H. Huang, First-principles calculation of the air-water second virial coefficient, Int. J. Thermophys. 28 (2) (2007) 556–565, https://doi.org/10.1007/s10765-007-0197-8.
[64] A. Oertel, R. Emmanuel, P. Drach, Assessment of predicted versus measured thermal comfort and optimal comfort ranges in the outdoor environment in the temperate climate of Glasgow, UK, Build. Serv. Eng. Res. Technol. 36 (4) (2015) 482–499, https://doi.org/10.1177/0143624414564444.
[65] S. Becker, O. Potchter, Y. Yaakov, Calculated and observed human thermal sensation in an extremely hot and dry climate, Energ. Buildings 35 (8) (2003) 747–756, https://doi.org/10.1016/S0378-7788(02)00228-1.
[66] M. Bruse, H. Fleer, Simulating surface-plant-air interactions inside urban environments with a three dimensional numerical model, Environ. Model Softw. 13 (3–4) (1998) 373–384, https://doi.org/10.1016/S1364-8152(98)00042-5.
[67] C.J. Willmott, On the validation of models, Phys. Geogr. 2 (2) (1981) 184–194, https://doi.org/10.1080/02723646.1981.10642213.
[68] L.C. Castro, K.M. Degues, M.G. Cypriano, M.R. Rocha, O.R.K. Montedo, E. Angioletto, Evaluation of the thermal performance of different cold materials for urban paving, Ceramica 63 (366) (2017) 203–209, https://doi.org/10.1590/0366-69132017633662063.